A Graph RAG Approach to Enhance Explainability in Dataset Discovery

Composite Structures 209 (2019) 45–59

Contents lists available at ScienceDirect

Composite Structures

journal homepage: www.elsevier.com/locate/compstruct

Improving the flexural capacity of extrudable foamed concrete with glass-fiber bi-directional grid reinforcement: An experimental study

Devid Falliano[a], Dario De Domenico[a,*], Giuseppe Ricciardi[a], Ernesto Gugliandolo[b]

[a] Department of Engineering, University of Messina, Contrada Di Dio, 98166 Sant'Agata, Messina, Italy
[b] G. Gugliandolo s.r.l., Via Galileo Galilei, 98100 Messina, Italy

ARTICLE INFO

Keywords:
Extrudable foamed concrete
Lightweight concrete
Glass fiber grid reinforcement
Curing conditions
Polymer fibers
Indirect tensile strength

ABSTRACT

A wide experimental campaign of 40 three-point-bending tests on small-scale foamed concrete beams in the low-to-medium density range (400–800 kg/m^3) is presented. The considered "extrudable foamed concrete" can keep its dimensional stability at fresh state. In order to increase the mechanical characteristics while preserving lightweight properties associated with the low densities, bi-directional grids of glass fibers are placed close to the bottom external face of the beams. Additionally, the use of short polymer fibers embedded within the cementitious matrix is investigated. Different specimen characteristics are explored, including: three curing conditions, three target dry densities, and two fiber contents. The presence of bi-directional grids increases the bending strength values for all the examined conditions: for 400 kg/m^3 the increase is up to 1700%, and for higher densities is, on average, 175%. The curing condition affects the failure mode: specimens cured in water with densities higher than 600 kg/m^3 exhibit a premature failure of the grid reinforcement without separation from the concrete substrate, whereas in those cured in air and cellophane typical bond failures with detachment occur. Only for densities of 800 kg/m^3 the further addition of short polymer fibers produces non-negligible flexural strength increase of 31%, on average.

1. Introduction

In order to achieve concrete elements with low self-weight, the addition of preformed foam is a usual and effective strategy that can be employed so as to obtain the so-called foamed concrete. This combined material also may include other ingredients like fly ash or silica fume as partial replacement of the traditional aggregates to enhance the mechanical properties [1]. The possibility of re-using slags of by-products of other manufacturing processes is also convenient from a sustainability point of view. As an example, electric arc furnace slag [2,3], recycled glass, or foundry slag [4] could be employed.

The use of foamed concrete is particularly attractive due to lightweight properties, thermal insulating features especially when low densities are employed [5,6], fire resistance [7], good acoustic shielding properties [8] and workability [9] as compared to traditional concrete. However, foamed concrete, especially in the low-to-medium density range (less than 1600 kg/m^3), is characterized by a relatively low strength [10]. In such low-density range foamed concrete can be a useful material for realizing non-structural elements and partitions in buildings, substrates in road construction [11], industrial concrete floors [12], whereas for higher densities it might be used for structural applications like composite walling systems [13]. Ultra-low density foamed concrete (less than 500 kg/m^3) can also have further interesting applications as filling material in interspaces, excavations, cavities and underground channels. However, these ultra-low density specimens may suffer from potential risk of instability due to separation of solid and air phases in the concrete mix [14,15].

Experimental data reveal that the dry density plays a key role in the strength of foamed concrete, but also the water/cement and air/cement ratios have a crucial impact [16]. In the relevant literature, different authors have investigated the correlation between strength and such influencing parameters [17,18].

In order to enhance the mechanical behavior of foamed concrete while preserving lightweight properties associated with low densities, in the literature embedded short fiber inclusions of different nature (i.e., polypropylene, kenaf, steel, oil palm fiber) have been resorted to [19–24], and other types, like basalt and coconut fibers, have been employed in traditional (not lightweight) concrete elements [25,26] and could easily be extended to foamed concrete. These fibers are randomly distributed in the cementitious matrix during the mixing phase; they not only increase the strength of the material, but also reduce drying shrinkage phenomena to a large extent. Instead, the study

* Corresponding author.
E-mail address: dario.dedomenico@unime.it (D. De Domenico).

https://doi.org/10.1016/j.compstruct.2018.10.092
Received 16 July 2018; Received in revised form 11 October 2018; Accepted 25 October 2018
Available online 26 October 2018

Fig. 1. Qualitative comparison of cohesion and viscosity of extrudable (a, b) and classical (c, d) foamed concrete at the fresh state (specimen preparation with equal target dry density of 600 kg/m^3).

of reinforcement grids [27,28] to enhance the tensile strength of foamed concrete has not been as common as embedded short fiber inclusions. This shows similarities with the common Textile Reinforced Concrete (not lightweight) widely studied in the literature, see e.g. [29,30], to name just a few contributions in the field.

1.1. Goal of the paper and research significance

In line with this research subject, the aim of this paper is to present a set of experimental results of three-point-bending tests performed on small-scale foamed concrete beams in the low-to-medium density range. The specimens are reinforced through the placement of a bi-directional grid of glass fibers in the tensile zone to ensure increased flexural capacity. A further diffused reinforcement layout has been studied in which, in addition to the above bi-directional reinforcing mesh, short polymer fibers are embedded in the cementitious paste during the mixing phase. A broad experimental campaign including almost 40 tests has been conducted to investigate the dependence of the flexural capacity of foamed concrete upon: 1) dry density; 2) curing conditions; 3) reinforcement arrangement (either only bi-directional grids or combined grids with short fibers); 4) fiber content. Although various types of foaming agents exist that may be employed for the specimen preparation (e.g., synthetic or protein-based) [31], in this study only a protein-based foaming agent is adopted, which has been identified as the most suitable one in a previous experimental campaign [10]. Besides the evaluation of the flexural capacity gain produced by the different reinforcement strategies, specific comments will be also outlined regarding the failure mode of the specimens. It is observed that the failure mode is strongly influenced by the specimen characteristics and by the curing conditions.

The present contribution deals with a particular class of foamed concrete obtained by adding foam and viscosity enhancing agent (VEA) into the cement paste so as to achieve a peculiar and unconventional property of extrudability [32,33]. The motivation of studying these reinforcement arrangements and the structural performance of this fiber-reinforced extrudable foamed concrete derives from potential applications in the civil engineering field [34]. Indeed, in the authors' opinion this material could be used for infill walls of buildings, composite walling systems [35] or for industrial concrete floors. Although there are other studies from the literature that highlight the increase of the flexural capacity through fiber reinforcement grids, the novel contributions of this research work regard the following aspects: 1) the use of bi-directional grids in the ultra-low density foamed concrete elements (400 kg/m^3); 2) the effect of different curing conditions on the failure mode of the specimens and on the corresponding increase of flexural capacity; 3) the study of the interaction between two levels of reinforcement, namely glass-fiber bi-directional grids combined with embedded short polymer fibers; 4) in the latter combined reinforcement configuration, the use of high fiber contents (up to 5%), whereas most studies typically focus on a range from 0.2% to 1.5% of volume content.

2. Experimental campaign

The experimental campaign has comprised around 40 three-point-bending tests on small-scale foamed concrete beams. The prismatic specimens have dimensions of 40 × 40 × 160 mm according to the UNI EN 196-1 standards ("Methods for testing cement") and have been prepared for the determination of the flexural strength, and of the compressive strength. In particular, the flexural strength is investigated first through the three-point bending method. After the flexural test is concluded, compressive tests are carried out on halves of the prism broken, thus obtaining two compressive strength values for each prism.

2.1. Materials

All the specimens were prepared using Portland CEM I 52,5 R in accordance with the EN 197-1 standards in terms of mix proportions of the constituting elements. A protein-based foaming agent called Foamin C® (trademark name) has been used in the experimental campaign, which is a brown, liquid foaming agent with acidity PH equal to 6.6 and

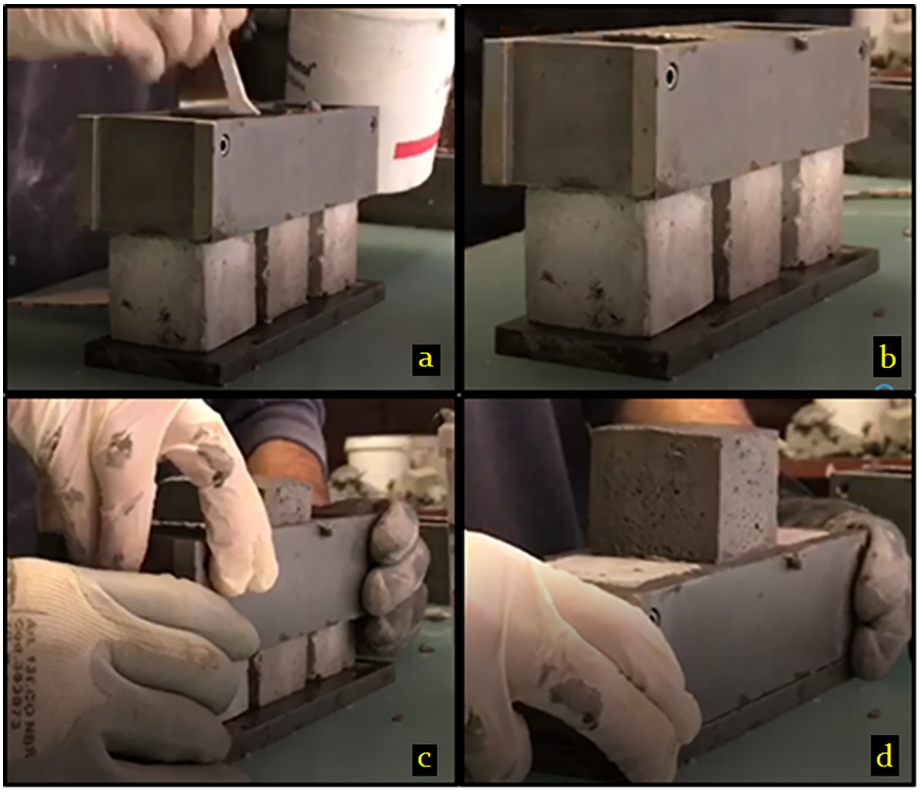

Fig. 2. Dimensional stability of the foamed concrete fresh paste during a rudimental extrusion process: a) filling of the steel formwork with cement fresh paste; b) end of the filling phase; c) extrusion phase; d) assessment of the fresh state dimensional stability.

specific weight 1.16 g/ml. A particular VEA was introduced in the cementitious paste to improve the cohesion and viscosity of the lightweight cement mix without deteriorating the workability of the material at its fresh state [32,33]. This additive produces the peculiar characteristic of "extrudability", as the material keeps the dimensional stability at its fresh state – hereinafter this material will be referred to as extrudable foamed concrete. Some images highlighting this peculiar behavior in comparison with classical (conventional – non extrudable) foamed concrete are displayed in Fig. 1. In particular, in Fig. 2 the ability of the foamed concrete paste to keep its shape at the fresh state is illustrated. To this end, a rudimental extrusion process has been obtained through the pressure exerted by a piston represented by a hardened cubic specimen underlying the fresh sample [33]. This is a distinctive peculiarity of this extrudable version of foamed concrete because a classical foamed concrete sample in a similar situation would expand laterally and would gradually collapse. Considering this peculiarity, the production process could proceed without the need of formwork, which is particularly convenient for prefabricated elements, thus speeding up the overall construction times.

Table 1
Geometric and mechanical characteristics of fiberglass mesh.

Reinforcement type	Weight per unit area (g/m^2)	Mesh spacing (mm × mm)	Content of resin (%)	Alkali resistance (%)	Ultimate tensile strength (kN/m)[†]
Fiberglass mesh (bi-directional)	125	10 x 10	14	56	25

[†] Standard basis: JG 149-2003.

The reinforcement elements consist of bi-directional glass-type fiber reinforcement grids and short polymer fibers as illustrated in Fig. 3. The main geometric and mechanical characteristics of the fiberglass mesh are listed in Table 1, while the ones pertinent to the polymer fibers are reported in Table 2.

Fig. 3. Glass fiber reinforcement bi-directional grid (a) and short polymer fibers (b, c).

Table 2
Geometric and mechanical characteristics of short polymer fibers.

Reinforcement type	Specific weight (kg/dm^3)	Appearance	Equivalent diameter (mm)	Fiber length (mm)	Ultimate tensile strength (MPa)[†]
Short polymer fibers	1.00	Macro fibers, wave shape	0.54	20	520

[†] Standard basis: ASTM C-1116; UNI 11039/1; UNI 11039/2.

2.2. Specimen preparation, mix proportions and curing conditions

By referring to the schematic stages illustrated in Fig. 4, some details on the specimen preparation are discussed in this subsection. The first step was the preparation of the cement paste. This was achieved by mixing cement, water and the particular VEA (in proportion 5% of the cement weight) to obtain the above-mentioned extrudability property (speed of around 3000 rpm for 1 min). Once a homogeneous paste is obtained, the foamed concrete was prepared by mixing this paste with preformed foam. The latter was produced through an appropriate foam generator. Within the generator, water and foaming agent (with a concentration of 3% of the water volume) are mixed with compressed air at a 3 bar pressure and introduced into the collector in which the foam is formed for dynamic turbulence. Using these parameters the obtained foam had a density of approximately 80 g/l. This foam is finally added to the paste and mixed at a speed of around 3000 rpm for 2 min until a homogeneous foamed concrete is obtained with a system of air voids in the microstructure. The foam content was varied depending on the target dry density. Three target dry densities were examined in this experimental campaign, namely 400, 600 and 800 kg/m^3, with a tolerance of ± 50 kg/m^3 – specimens outside this range were excluded from the experimental study. Besides the variability of the strength with the target dry density, in this study also the influence of the curing conditions on the ultimate behavior (peak load and collapse mode) was investigated. Overall, 37 series of specimens were prepared. Some of the specimens were without reinforcement so as to have a reference set of beams for comparative purposes. Some other beams were reinforced with glass-fiber bi-directional grids that were placed in the tensile zone of the specimens, precisely at around 4 mm distance from the external face, and covering the remaining height of the beam with additional foamed concrete. Finally, some other beams were prepared combining both the glass-fiber grids with short polymer fibers that were preliminarily embedded in the lightweight cementitious paste.

After de-moulding, the specimens were cured in three different conditions as reported in Fig. 5, namely: 1) in air at environmental temperature of (20 ± 3 °C) and relative humidity (RH) of 75%, which represents the worst configuration for achieving the flexural and compressive strength; 2) by wrapping the specimens within a cellophane sheet at a temperature of 20 ± 3 °C and RH of 75%. This is a conventional curing procedure employed in foamed concrete precast industry [4] to prevent significant evaporation of water during the curing process; 3) in water at a controlled temperature of 30 °C within a closed tank. For each curing conditions and for each fiber content three different specimens were prepared to achieve the three target dry densities. In this way, a set of almost 40 specimens were prepared. This wide database allowed us to compare the flexural strength and the corresponding compressive strength, in addition to the failure mode, of a set of specimens having different characteristics. Therefore, this experimental study has made it possible to highlight the effect of dry density, of curing conditions and of fiber content in addition to the glass-fiber bi-directional grid reinforcement on the flexural capacity of foamed concrete.

For each reinforcement arrangement and curing condition, a series of specimens were prepared having different densities. All the mix proportions are reported in Table 3. In particular, the mix design of each specimen analyzed in this study is documented in terms of water content w, foam content f and related ratios f/c, w/c and $(w + f)/c$, which are computed for each specimen, with c denoting the weight of cement. Moreover, the additive content a (in percentage of the cement weight) and the short fiber content rf (in weight per unit volume) are also listed in Table 3. As listed in Table 3, the water/cement ratio is assumed constant for all the tested specimens and equal to 0.30, in line with a previous experimental campaign carried out on classical (not

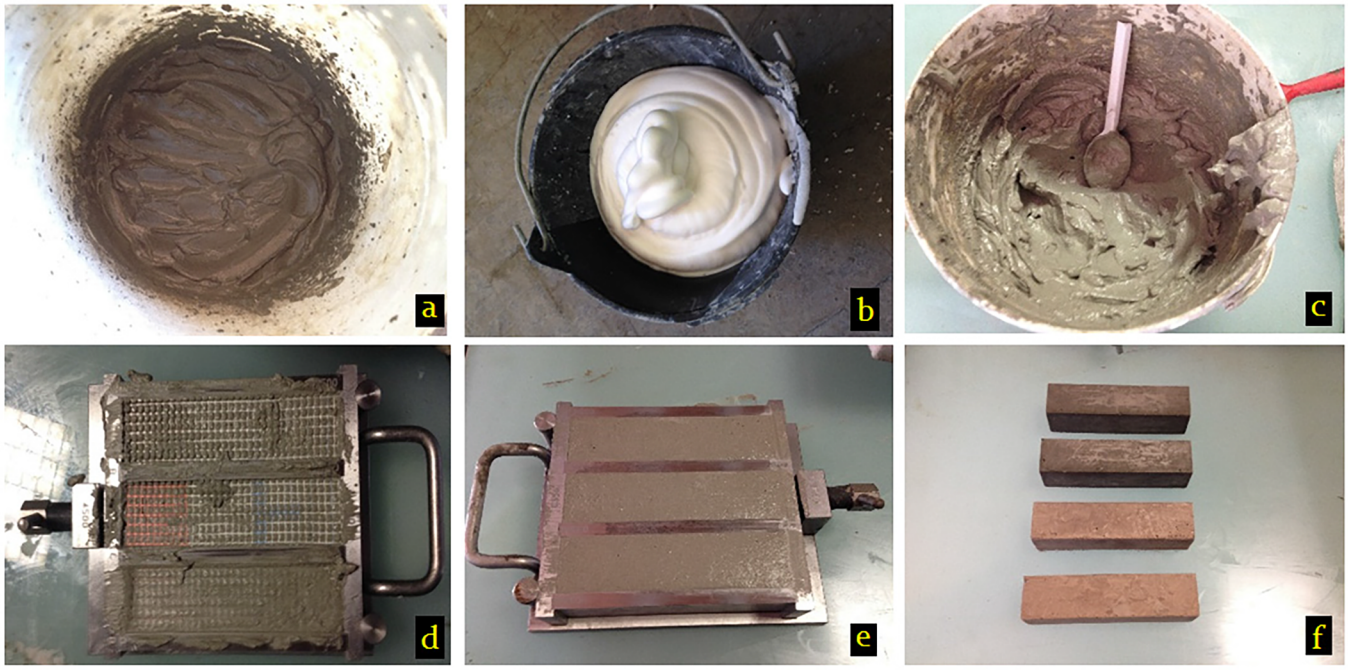

Fig. 4. Photographs of the specimen preparation of foamed concrete beams: a) mix of water, cement and VEA; b) preformed foam; c) paste obtained with a) + b); d) application of bi-directional reinforcement grids; e) covering of the reinforcement grid and completion; f) de-molding of the specimens.

Fig. 5. Curing conditions of some of the tested beams in air at environmental temperature (a), wrapped in cellophane sheet at environmental temperature (b), and in water at controlled temperature (c).

Table 3
Mix design of the tested specimens of foamed concrete.

mix no. †	Mix design								
	dry density γ_{dry} [kg/m^3]	cement c [kg/m^3]	water w [kg/m^3]	foam f [kg/m^3]	VEA additive a [%]	short fiber content rf [kg/m^3]	ratio 1 w/c	ratio 2 f/c	ratio 3 $(w+f)/c$
400U	408	319	96	181	5	–	0.3	0.57	0.87
600U	608	465	139	196	5	–	0.3	0.42	0.72
800U	825	648	194	182	5	–	0.3	0.28	0.58
400G	422	322	97	162	5	–	0.3	0.50	0.80
600G	625	477	143	180	5	–	0.3	0.38	0.68
800G	784	623	187	174	5	–	0.3	0.28	0.58
400GF2	443	330	99	162	5	18.3	0.3	0.49	0.79
600GF2	596	429	129	176	5	17.2	0.3	0.41	0.71
800GF2	778	619	186	186	5	19.2	0.3	0.30	0.60
400GF5	435	327	98	168	5	44.5	0.3	0.51	0.81
600GF5	598	431	129	180	5	43.0	0.3	0.42	0.72
800GF5	802	631	189	201	5	48.5	0.3	0.32	0.62

† The number denotes the target dry density of the mix (400, 600, 800 kg/m^3) and is followed by the beam type indicated with U (unreinforced), G (reinforced with grids), GF2 (reinforced with combined grids and short fiber at 2% content) and GF5 (reinforced with combined grids and short fiber at 5% content).

extrudable and not reinforced) foamed concrete specimens [10].

In addition to the dry densities for each specimen γ_{dry} (determined after the testing and after drying the specimen in an oven as described below), also the fresh density γ_f (at the preparation stage) and the wet density γ_{wet} (after 28 days in air curing conditions at natural humidity conditions) are computed and reported in Table 4. Considering the three above defined density values, it was then possible to calculate the water content of each specimen in air curing conditions as $w_a = 100\cdot(W_{wet} - W_{dry})/W_{wet}$ [%], and also the difference between fresh and wet density as percentage, i.e., $\Delta\gamma = 100\cdot(\gamma_f - \gamma_{wet})/\gamma_f$ [%]. As can be noted from Table 4, the fresh density ranged approximately from 600 to 1100 kg/m^3, the wet density from 500 to 1000 kg/m^3 and the dry density from 400 to 830 kg/m^3. The porosity listed in Table 4 was computed according to the simplified formula reported in [6], that is

$$\varepsilon = 1 - \frac{\gamma_{dry}}{\gamma_{solid}}$$

wherein γ_{solid} indicates the density of the cementitious matrix and was calculated on specimens prepared without foam (this value was equal to 1850 kg/m^3), while γ_{dry} denotes the dry density measured on the foamed concrete specimens. The latter density was evaluated after the

Table 4
Evaluation of density at different states of the specimens for air curing conditions.

series no.	fresh density γ_f [kg/m^3]	wet density γ_{wet} [kg/m^3]	density difference $\Delta\gamma$[%][1]	dry density γ_{dry} [kg/m^3]	porosity ε[%]	water weight ratio w_a[%][2]
#1U	609	502	17.57	408	77.94	18.72
#2U	835	750	10.18	608	67.13	18.93
#3U	1105	1015	8.14	825	55.40	18.72
#1G	620	510	17.74	422	77.17	17.19
#2G	865	780	9.83	625	66.20	19.83
#3G	1065	991	6.95	784	57.60	20.85
#1GF2	635	530	16.53	443	76.07	16.48
#2GF2	819	730	10.87	596	67.78	18.35
#3GF2	1073	975	9.13	778	57.93	20.17
#1GF5	614	519	15.47	435	76.49	16.18
#2GF5	805	725	9.94	598	67.66	17.47
#3GF5	1062	975	8.19	802	56.65	17.74

[1] Difference between fresh density and wet density (after 28 days).
[2] Computed as the difference between the dry weight and the wet weight of the specimen over the wet weight.

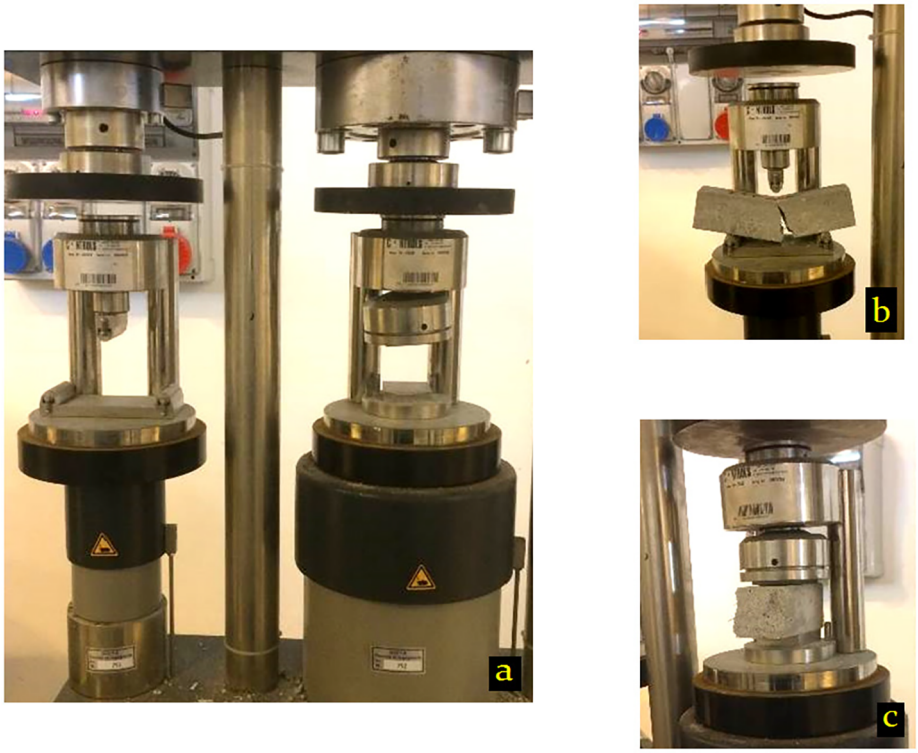

Fig. 6. Photographs of the testing equipment used in the experimental campaign: a) CONTROLS test frame model 65-L1301/FR; b) close-up detail of the three-point bending test; c) close-up detail of the compression test on halves of broken prism.

tests and after placing the specimens within an oven at 110 °C until a constant weight was reached. Although the above formula is rather simplified, it has been demonstrated in earlier studies to be accurate enough to give a reasonable estimate of the porosity against more accurate methods like those commonly employed in the microstructural analysis (e.g., X-ray computerized tomography and 3D image processing) [36].

2.3. Testing conditions

The prismatic specimens were tested at 28 days from casting (in the three above-specified curing conditions) under three-point-bending according to UNI EN 196-1 standards. A CONTROLS test frame model 65-L1301/FR was used. This testing equipment is composed of a twin column rigid steel construction since it allows both compression and indirect tensile test, as displayed in Fig. 6. The frame for the indirect tensile test has 15 kN load capacity, while that related to the compression test 250 kN. For the indirect tensile strength the load was applied at a rate of 50 N/s, while for the compression test the load rate was 2400 N/s in compliance with the tolerances allowed by UNI EN 196-1 standards. For each test the peak load was recorded and then the compressive and indirect tensile strength were calculated. For the compressive test, the halves of the prism broken in the indirect tensile test were placed on two platens of 4 cm side in accordance with the specifications of the UNI EN 196-1 standards.

3. Extrudable foamed concrete beams without reinforcement

In this Section we report the indirect tensile strength f_t and compressive strength values R_c measured on the group of foamed concrete specimens without reinforcement. These values are assumed as reference for assessing the increase of the strength induced by the different reinforcement strategies discussed in the following sections. Thus, they are assumed as benchmark data for comparative purposes. In Table 5, the experimental strength values are listed for all the tested specimens in the three considered curing conditions, namely in air, cellophane, and water, respectively. The specimens are labelled with different numbers, and the letter "U" associated with each specimen in Table 5 indicates the un-reinforced configuration of this set of beams. Considering that the compressive strength was determined on two

Table 5
Experimental indirect tensile strength and compressive strength for each series of the specimens without reinforcement.

curing conditions	series no.	dry density γ_{dry} [kg/m^3]	indirect tensile strength f_t [MPa]	mean compressive strength R_t [MPa]	st. dev. compressive strength σ_{Rc} [MPa]	COV strength COV_{Rc}
air	#1U	413	0.09	1.665	0.092	0.055
	#2U	611	1.09	6.21	0.113	0.018
	#3U	814	2.15	12.23	0.424	0.035
cellophane	#4U	413	0.12	1.71	0.099	0.058
	#5U	609	1.23	6.43	0.035	0.005
	#6U	824	2.40	11.87	0.481	0.040
water	#7U	398	0.10	1.52	0.134	0.088
	#8U	604	1.24	6.14	0.042	0.007
	#9U	838	2.53	12.07	0.24	0.020

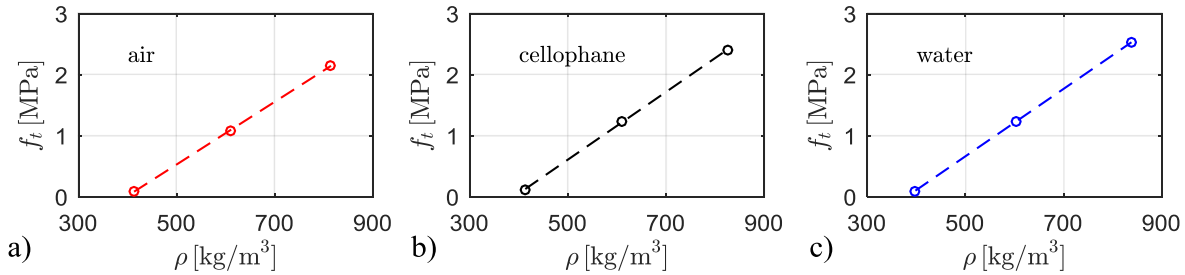

Fig. 7. Experimental indirect tensile strength for foamed concrete beams without reinforcement and different curing conditions: a) air; b) cellophane; c) water.

halves of the broken prismatic specimen, the arithmetic mean is computed and reported in the Table, along with the standard deviation σ_{Rc} and the coefficient of variation (COV) of the two sets of measures COV_{Rc}.

The effect of dry density and curing conditions on the indirect tensile and compressive strength can be thus analyzed. In the following subsections a series of graphs are constructed in terms of indirect tensile and compressive strength values versus the actual dry density for different curing conditions. The experimental data, indicated by markers in the plots, are accompanied by the corresponding linear regression curves that are found via a least-square minimization procedure to give some design indications and conclusions based on the present experimental study.

3.1. Effect of dry density

In Fig. 7 the indirect tensile strength values f_t are reported versus the dry density of the specimens. It is noted that the f_t values increase almost linearly with increasing the dry density in the range of densities examined in this experimental campaign – the linear regression curve describes almost perfectly the experimental data. The transition from 400 kg/m^3 to 600 kg/m^3 results in a dramatic increase of the tensile strength, and this is due to the very low strength associated with the lowest dry densities. Without any kind of reinforcement, these ultra-low dry densities are associated with a modest bearing capacity. Instead, the transition from 600 kg/m^3 to 800 kg/m^3 implies a percentage relative increase of around 85–100% of the tensile strength value. Similar trend is observed for the compressive strength values obtained on two halves of the broken prismatic specimen and reported in Fig. 8. A comparable percentage increase is computed when passing from 600 kg/m^3 to 800 kg/m^3, while more than 250% increase is obtained passing from 400 kg/m^3 to 600 kg/m^3.

3.2. Effect of curing conditions

In addition to the effect of dry density, the influence of the curing conditions of the specimens on the achievement of the final strength values has also been investigated. In Fig. 9 the variability of the indirect tensile strength values f_t with the curing conditions is illustrated for the three target dry densities considered. It is noted that, as normally expected, the water curing conditions are associated with the highest indirect tensile strength values, although this trend is not confirmed for the specimens having a target dry density of 400 kg/m^3 – but this is justified by the very low values of the strength measured in the lowest target dry densities. However, the differences observed between the three curing conditions are not considerable for the beams without reinforcement: around 1–5% of increase comparing specimens cured in cellophane and water, and approximately 10–15% of increase comparing specimens cured in air and cellophane. Therefore, comparing the worst and the best curing condition we have measured a percentage increase of around 15–18% for the indirect tensile strength.

Even more negligible are the differences related to the compressive strength values R_c associated with the three curing conditions, as reported in Fig. 10. The cellophane curing conditions seemingly represent the best ones for the achievement of the highest compressive strength values, and this result is quite in line with a previous experimental campaign focused on the compressive strength of classical (not extrudable) foamed concrete [10].

4. Beams reinforced with bi-directional grids of glass fibers

In this section, the experimental results pertaining to the foamed concrete beams reinforced with bi-directional grids of glass fibers are reported. The values of the indirect tensile strength f_t and compressive strength values R_c for the examined specimens are all listed in Table 6. Here, the nomenclature G stands for grid reinforcement. Unlike the previous set of un-reinforced foamed concrete beams discussed above, for this class of reinforced specimens the two halves of the prismatic beam were not always in proper conditions to be used for the subsequent compressive strength tests. This was due to the specific failure mode of these reinforced beams in which a significant portion of the concrete cover separated from the rest of the specimen – this will be better clarified in the following discussions by reporting some photographs of the collapsed beams. In almost all the cases, only one of the two halves was not excessively damaged during the three-point-bending test, thus it was not possible to measure a couple of compressive strength values for each specimen type and, for this reason, the standard deviation σ_{Rc} and the coefficient of variation COV_{Rc} are omitted for this set of specimens. As for the un-reinforced beams, the same effect of dry density and curing conditions on the indirect tensile

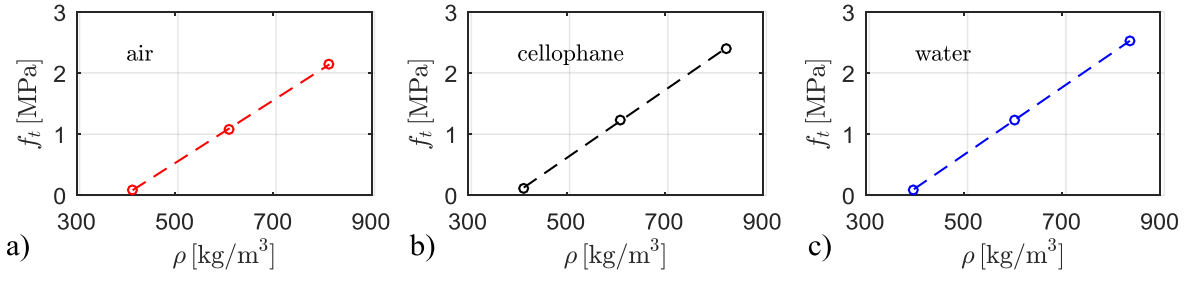

Fig. 8. Experimental mean compressive strength on halves of broken prismatic foamed concrete beams without reinforcement and different curing conditions: a) air; b) cellophane; c) water.

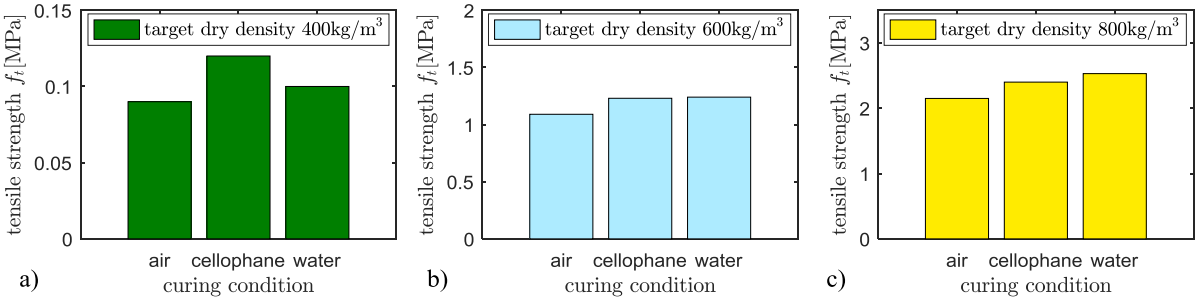

Fig. 9. Effect of the curing conditions on the experimental indirect tensile strength values for foamed concrete beams without reinforcement: a) 400 kg/m^3; b) 600 kg/m^3; c) 800 kg/m^3.

and compressive strength is illustrated below through a series of plots.

Using the same format of the plots adopted for the un-reinforced beams, in Fig. 11 the indirect tensile strength values f_t are reported versus the dry densities of the specimens. By inspection of the experimental data (markers reported in the plot), a linear increase is observed for the air and cellophane curing conditions, while for water curing conditions the trend is different. This result will be clarified in the next subsection regarding the influence of the curing conditions. By comparing this plot with the previous ones relevant to the un-reinforced beams, it is evident that there is a marked increase of the indirect tensile strength values due to the placement of the bi-directional grid of glass-fiber reinforcement. Similar to the un-reinforced case, we can compute the percentage increase when passing from 400 kg/m^3 to 600 kg/m^3 and from 600 kg/m^3 to 800 kg/m^3 for air and cellophane curing conditions: on average, this percentage increase is around 115% and 30%, respectively. For water curing conditions the transition from 400 kg/m^3 to 600 kg/m^3 implies a significant increase of strength, whereas passing from 600 kg/m^3 to 800 kg/m^3 this trend is not confirmed in that the strength is almost constant. It will be demonstrated below that for these testing conditions (water curing and dry density of 600–800 kg/m^3) the ultimate load is specifically related to the strength of the grid reinforcement where the rupture takes place, and not particularly affected by the foamed concrete strength.

The water curing conditions are associated with the worst indirect tensile strength values for the beams with grid reinforcement, see Fig. 12. This is due to the degradation of the mechanical characteristics of the grid induced by the water curing conditions, which cause a premature rupture of the grid at the mid-span soffit of the beam at ultimate conditions – see below for photographs of the collapse mechanism. This becomes manifest at typical densities of 600–800 kg/m^3 analyzed in this experimental campaign. Also at lower densities, namely for the specimens having a target dry density of 400 kg/m^3, the mechanical characteristics of the reinforcement grid are negatively affected by the water curing conditions: this is clearly noted in the left part of Fig. 12 wherein the lowest strength values are associated with water curing conditions. However, in contrast to the higher densities, the above-mentioned premature grid rupture does not occur because of the relatively low bond strength of the surrounding foamed concrete for target dry density of 400 kg/m^3. In this case, although the degradation of the grid reinforcement in water curing conditions occurs, the failure is governed by the bond strength of the foamed concrete. Indeed, typical bond failure with detachment of concrete substrate from reinforcement takes place – see below for more details on the failure mode. For these cases, further increase of the amount of grid or improvement of its properties would not necessarily result in a higher flexural capacity.

Since the ultimate indirect tensile strength is not ascribed to the foamed concrete, but mainly to the interaction between reinforcement grid and concrete substrate, a preferable curing condition between air and cellophane cannot be clearly identified, as the corresponding strength values do not follow a very clear trend for all the target dry densities as shown in Fig. 12 – indeed for 800 kg/m^3 cellophane is

Table 6
Experimental indirect tensile strength and compressive strength for each series of the specimens with glass-fiber bi-directional grid reinforcement.

curing conditions	series no.	dry density γ_{dry} [kg/m^3]	first-crack tensile strength f_{tc} [MPa]	rupture tensile strength f_t [MPa]	compressive strength R_c [MPa]
air	#1G	443	0.05	2.46	1.85
	#2G	647	2.39	4.51	n.a.†
	#3G	803	2.70	4.98	11.88
cellophane	#4G	417	0.047	1.88	1.99
	#4.1G	388	0.04	1.70	n.a.†
	#5G	611	2.32	4.35	n.a.†
	#6G	785	2.66	6.17	12.31
water	#7G	407	0.12	1.35	1.62
	#8G	618	2.27	3.44	n.a.†
	#9G	765	2.44	3.10	12.78

† Not available result due to the collapse mode in three-point-bending test that has affected also both the halves of the corresponding beams to be used for the compression test.

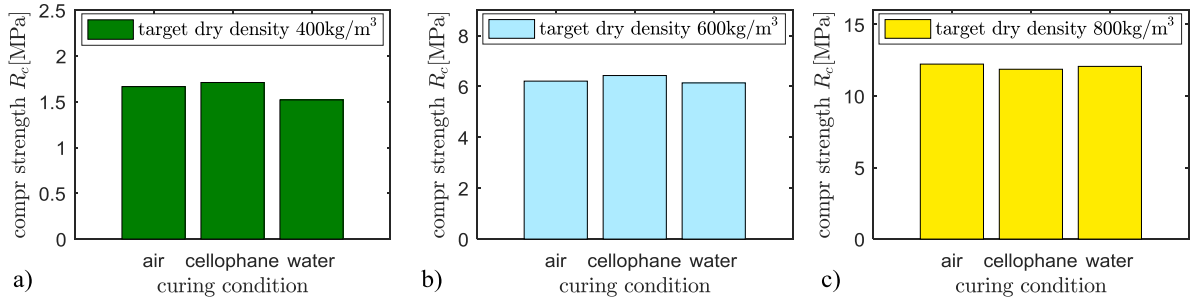

Fig. 10. Effect of the curing conditions on the experimental compressive strength values for foamed concrete beams without reinforcement: a) 400 kg/m^3; b) 600 kg/m^3; c) 800 kg/m^3.

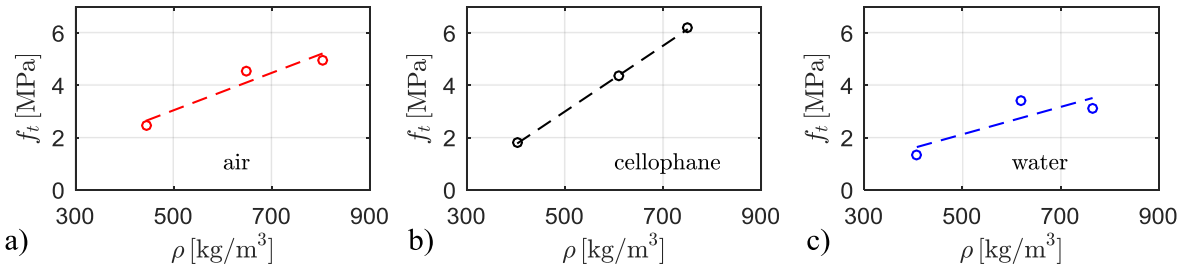

Fig. 11. Experimental indirect tensile strength for foamed concrete beams with glass-fiber bi-directional grid reinforcement and different curing conditions: a) air; b) cellophane; c) water.

better than air, for 400 kg/m^3 air is better than cellophane, and for intermediate situations at target dry densities of 600 kg/m^3 air and cellophane are comparable.

As said above, the curing conditions play a key role in the development of the failure mode of the beams reinforced with bi-directional grids of glass fibers. To demonstrate this, in Figs. 13 and 14 we report two typical failure modes of beams cured in air (or cellophane, as they are characterized by the same ultimate behavior) and in water, respectively. Failure modes for other beams with the same characteristics are qualitatively similar and are not reported for brevity.

Shown in these figures is the force–time plot and, for 4 representative force levels denoted with letters from A to D, the corresponding crack pattern. It is noted that the beams fail in two different manners depending on the curing conditions. With regard to beams cured in air (or in cellophane), a typical example of which is shown Fig. 13, a first-crack load (corresponding to a first-crack stress f_{tc}) is reached at point A, and this may be related to the tensile strength of the foamed concrete material. Indeed, this load is approximately equal to the one obtained for the foamed concrete beam without reinforcement as discussed in Section 3 (corresponding to a so-called un-reinforced tensile strength f_{tu}). Beyond this load point A, the force level decreases until the bi-directional grid of glass-fiber reinforcement is entirely involved in the tensile resistance, point B, and this implies the first crack propagates throughout the beam height up to the grid level and further cracks develop subsequently. From this stage onwards the force rises linearly with time (points B-C-D), which means that the beam can withstand further load increase, and the crack widths increase accordingly. The forces in this second stage are entirely resisted by the glass-fiber bi-directional grid reinforcement and transmitted to the surrounding concrete through bond stress mechanisms. This stress transfer mechanism is evidenced by the crack path illustrated in Fig. 13C. This mechanism proceeds up to point D wherein the bond strength of the foamed concrete is reached and the collapse occurs suddenly with the concrete cover separation as highlighted in Fig. 13D. Quite different is the collapse mechanism of the beams cured in water, a representative example of which is reported in Fig. 14. Although the initial stages of development of first-crack and subsequent load decrease (points A-B) are qualitatively the same as discussed above, the second stage of the test exhibits some notable differences. It is true that the trend is linear up to the failure like the in the previous beam cured in air, but the stress transfer mechanism from the glass-fiber bi-directional grid reinforcement to the surrounding foamed concrete does not develop entirely – this is evidenced by the almost vertical trend of the cracks from point B to D through C. This is due to the fact that the grid reinforcement reaches its ultimate tensile strength prematurely. This is clearly highlighted in Fig. 14D where the fiber rupture can be noted at the mid-span beam soffit. As anticipated above, this premature failure of the reinforcement is ascribed to the curing conditions in water, which affect the mechanical characteristics of the glass fiber. This hypothesis is corroborated by the observation of the indirect tensile strength values obtained for beams #8G (target dry density 600 kg/m^3) and #9G (target dry density 800 kg/m^3). Despite the higher value of dry density, the f_t value for the latter beam is slightly lower than the former: indeed, the ultimate tensile strength is mainly related to the grid reinforcement strength, in both cases negatively influenced by the water curing conditions, irrespective of the foamed concrete strength value that may be higher for increasing dry densities.

The ratio between the first-crack tensile strength of beams with reinforcement f_{tc} and the ultimate tensile strength of the un-reinforced beam f_{tu}, shown in Fig. 15 for the different densities and curing conditions, is nearly comprised between 0.5 and 2. This corroborates the hypothesis of stress mechanism described above, and confirms that the first-crack load is entirely ascribed to the foamed concrete strength as if the beam were un-reinforced.

In Fig. 16 we report the ratio between the ultimate to the first-crack tensile strength values f_t/f_{tc}, which is an indicator of the flexural capacity increase achieved by the reinforcement grid of glass fibers. As can be seen, for the reasons stated above in the water curing condition the lowest increases are accomplished, while in cellophane and air the trend is mixed and is also variable depending on the dry density (higher for air in the lowest density, higher for cellophane in the highest density, and almost comparable for the intermediate one).

Furthermore, for the target dry density of 400 kg/m^3 the observed increase is enormous (more than 40 times higher than the first-crack load). This result makes the proposed reinforcement strategy an effective method for obtaining an offset between ultra-lightweight

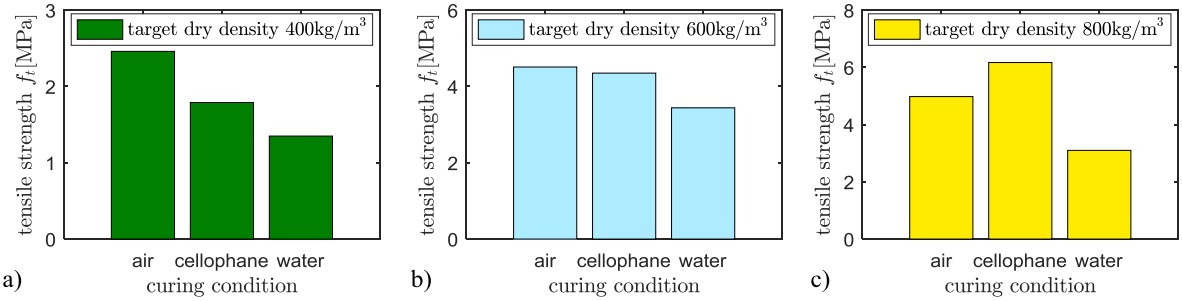

Fig. 12. Effect of the curing conditions on the experimental indirect tensile strength of foamed concrete beams with glass-fiber bi-directional grid: a) 400 kg/m^3; b) 600 kg/m^3; c) 800 kg/m^3.

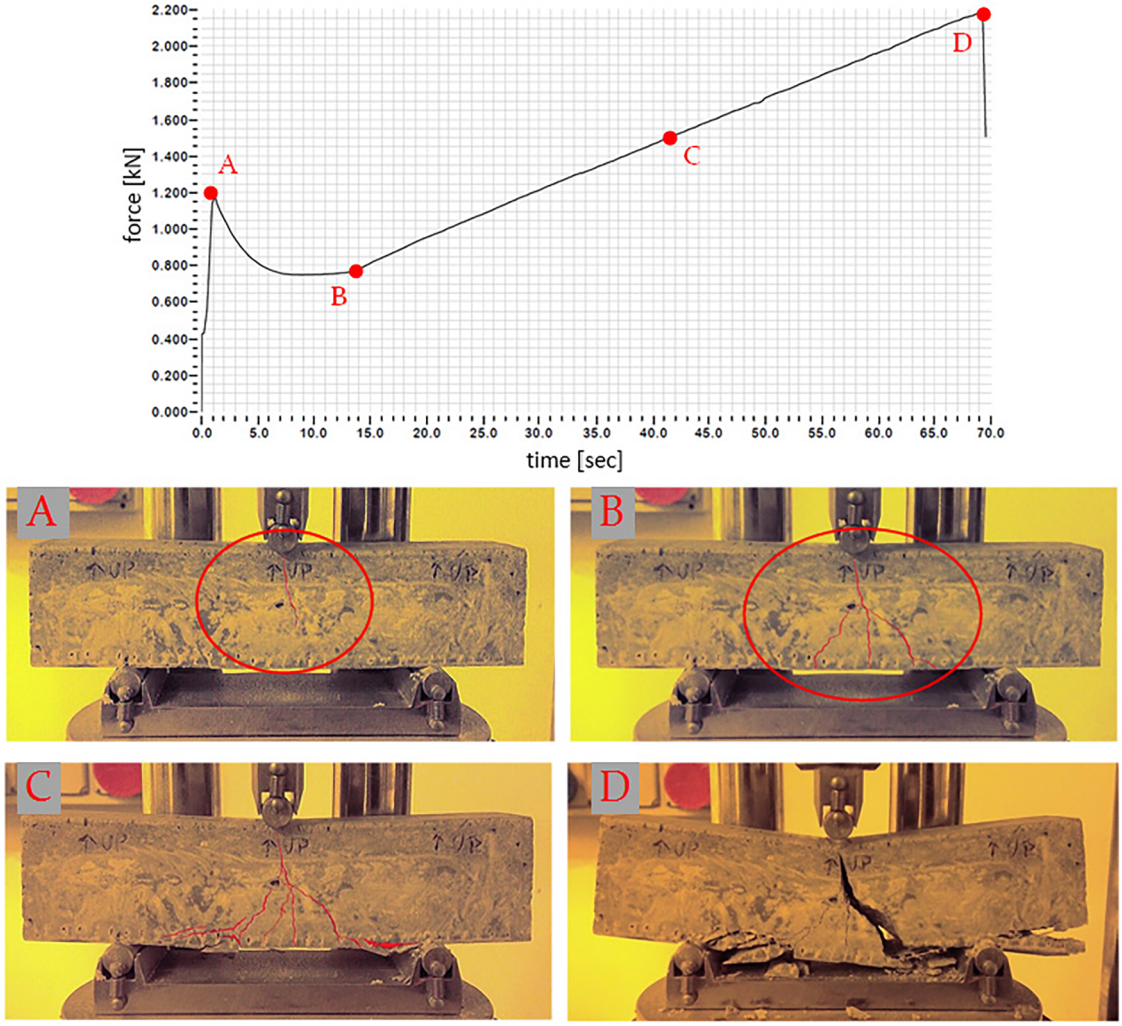

Fig. 13. Load-versus-time graph of beam #3G cured in air (top) and failure mode progression at different load steps (bottom) – typical bond failure with detachment of concrete substrate from reinforcement.

properties of foamed concrete and acceptable strength characteristics that cannot be achieved at such very low densities. At higher dry densities of 600 and 800 kg/m^3, although the increases are lower than the low density case by virtue of the higher strength values of the foamed concrete without reinforcement, the ultimate load is nearly twice as much as the first-crack load. Thus, the proposed reinforcement strategy is convenient for the entire range of target dry densities analyzed in this experimental campaign.

The previous observations are based on the indirect tensile strength values. The proposed reinforcement arrangement is specifically developed to improve the flexural capacity of foamed concrete, in line with the scope of the present paper. As expected, no considerable enhancement of the compressive strength is obtained as the values of the compressive strength obtained on the (non-damaged) halves of the prismatic beams, which are reported in Fig. 17, are not particularly higher than the previous results shown in Fig. 10 for un-reinforced specimens.

5. Beams reinforced with glass-fiber bi-directional grids combined with embedded short polymer fibers

In this section we present the experimental results concerning the foamed concrete beams with combined glass-fiber bi-directional grids reinforcement and short polymer-type fibers embedded in the cementitious paste. The motivation for introducing short polymer fibers in addition to the reinforcement grids is to investigate the possible interaction between the two levels of reinforcement. Indeed, the short fibers might improve the bond resistance of the surrounding concrete to delay the separation of the reinforcement grid so as to achieve higher ultimate flexural capacity. Two different contents of the short polymer fibers were analyzed, namely 2% and 5% in volume. Thus, 18 specimens were prepared, each corresponding to a given fiber content and curing condition for the three different target dry densities of the present experimental study.

In Fig. 18 the indirect tensile strength values are plotted against the target dry density for air, cellophane and water curing conditions, respectively, and for the 2% fiber content. The introduction of short fibers does not alter the linear trend of the flexural capacity with the dry density already noted for the other classes of specimens. Passing from 400 kg/m^3 to 600 kg/m^3 the percentage increase of the indirect tensile strength is 75% (averaged value on all the three curing conditions); instead, from 600 kg/m^3 to 800 kg/m^3 the increase is, on average, of 74%. There are, however, some variations from case to case depending on the specific curing conditions. Also in this case, the water curing conditions are associated with the lowest values of tensile strength, whereas cellophane and air yield rather comparable strength results, especially for the lower densities analyzed in this study. The specific values of the indirect tensile strength for each specimen at 2% fiber

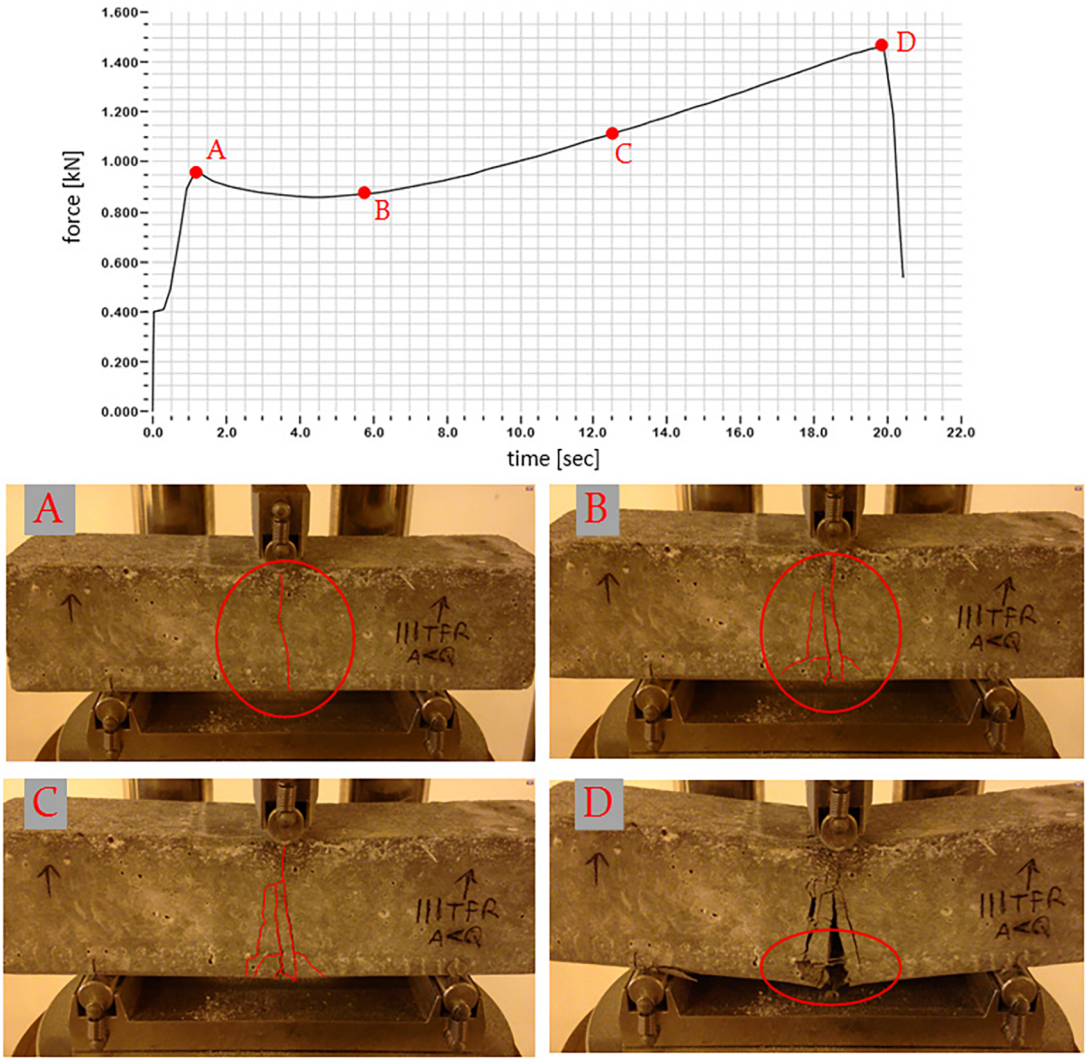

Fig. 14. Load-versus-time graph of beam #8G cured in water (top) and failure mode progression at different load steps (bottom) – typical rupture of the glass-fiber grid reinforcement.

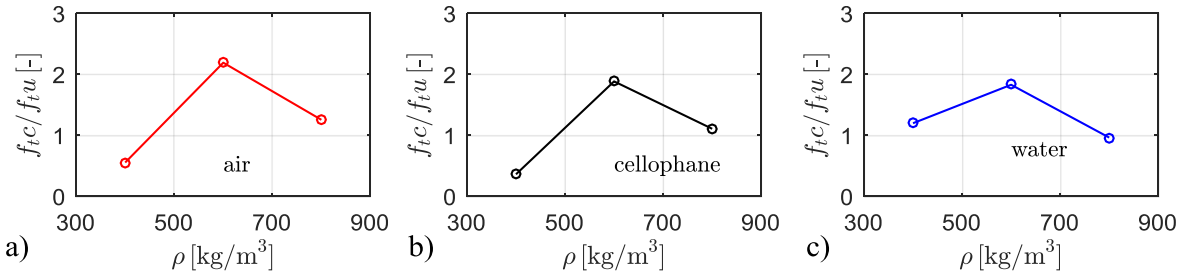

Fig. 15. Ratio of the first-crack tensile strength of beams with bi-directional glass-fiber grid reinforcement f_{tc} over the ultimate tensile strength of the un-reinforced beams f_{tu} for curing conditions in: a) air; b) cellophane; c) water.

content are listed in Table 7.

A further addition of fibers up to 5% in volume was analyzed in order to check whether or not this further fiber increase corresponds to higher flexural capacity correspondingly. Relevant results for 5% fiber content are shown in Fig. 19 and listed in Table 8. Quite similar conclusions to the previous case about the linear increase with the increasing dry densities can be drawn. An average increase of 81% is observed when passing from 400 kg/m^3 to 600 kg/m^3, and an average increase of 65% from 600 kg/m^3 to 800 kg/m^3. Also in this case the water curing conditions are the worst in terms of achievement of flexural capacity. Furthermore, by comparing the graphs illustrated in Figs. 18 and 19, as well as the corresponding values listed in Tables 7 and 8, it emerges that the additional 3% fiber content do not led to a significant increase of the tensile strength values in comparison with the 2% fiber content results, and the improvements are however rather negligible, not to say null. Thus, it is evident that beyond a certain amount of fibers, the interaction between the two levels of reinforcement is not improved any more. This result suggests to limit the fiber content, when used in conjunction with glass-type bi-directional grid reinforcement, to within 2%.

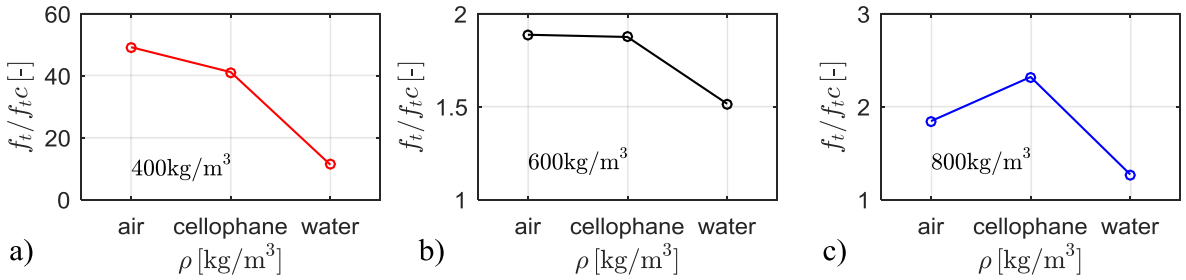

Fig. 16. Ratio of the ultimate f_t to first-crack f_{tc} tensile strength values of beams with bi-directional glass-fiber grid reinforcement for: a) 400 kg/m^3; b) 600 kg/m^3; c) 800 kg/m^3.

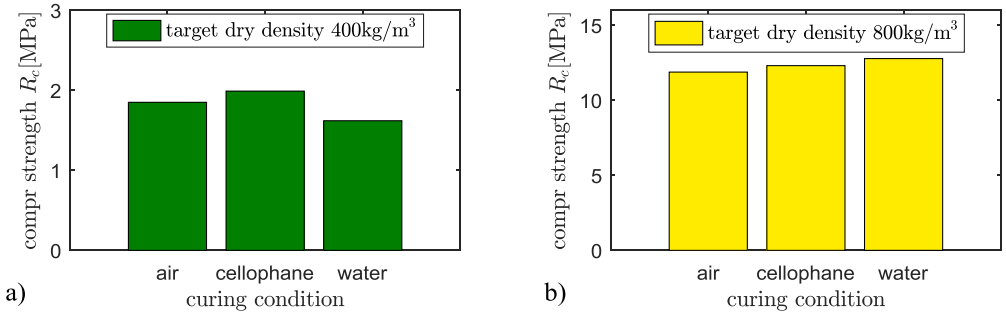

Fig. 17. Effect of the curing conditions on the experimental compressive strength values for foamed concrete beams with bi-directional glass-fiber grid reinforcement: a) 400 kg/m^3; b) 800 kg/m^3.

6. Comparison and discussion

Based on the results presented in the foregoing sections, in this short paragraph we discuss the comparison among the different reinforcement arrangements of the specimens. In Fig. 20 three comparative histograms are constructed and presented summarizing the indirect tensile strength results for the different target dry densities, the different curing conditions and the different reinforcement strategies analyzed in this experimental study. We do not report the analogous comparative histograms for the compressive strength values for the following reasons: 1) these values are not available for some of the reinforced specimens due to the difficulties in extracting undamaged halves of the beams after the indirect tensile test that may be representative for a compression test; 2) the reinforcement strategies presented in this study are specifically concerned with the improvement of the flexural capacity of the foamed concrete beams, therefore a corresponding enhancement of the compressive strength is not expected and, indeed, has not been observed in the few cases listed above.

Overall, with every reinforcement configuration we obtain a marked increase of the flexural capacity in comparison with the un-reinforced foamed concrete beams. The presence of the glass-fiber bi-directional grid reinforcement plays a major role in enhancing the indirect tensile strength of the beams. In water curing conditions the increase of flexural capacity achieved by the glass-fiber grids is reduced as compared to the other curing conditions for the reasons clarified above. This is particularly marked at the higher dry densities of 800 kg/m^3 where the increase is just of 20% as compared to the un-reinforced beam, whereas at low-medium densities of 600 kg/m^3 the increase is still evident and is

Table 7
Experimental indirect tensile strength and compressive strength for specimens with glass-fiber grids combined with short polymer fibers (2% in volume).

curing conditions	series no.	dry density γ_{dry} [kg/m^3]	rupture tensile strength f_t [MPa]	compressive strength R_c [MPa]
air	#1GF2	447	2.53	n.a.†
	#2GF2	604	4.51	n.a.†
	#3GF2	803	6.75	10.39
cellophane	#4GF2	442	2.56	n.a.†
	#5GF2	598	4.35	n.a.†
	#6GF2	752	7.72	12.60
water	#7GF2	439	1.94	n.a.†
	#8GF2	586	3.44	n.a.†
	#9GF2	780	6.24	11.34

† Not available result due to the collapse mode in three-point-bending test that has affected also both the halves of the corresponding beams to be used for the compression test.

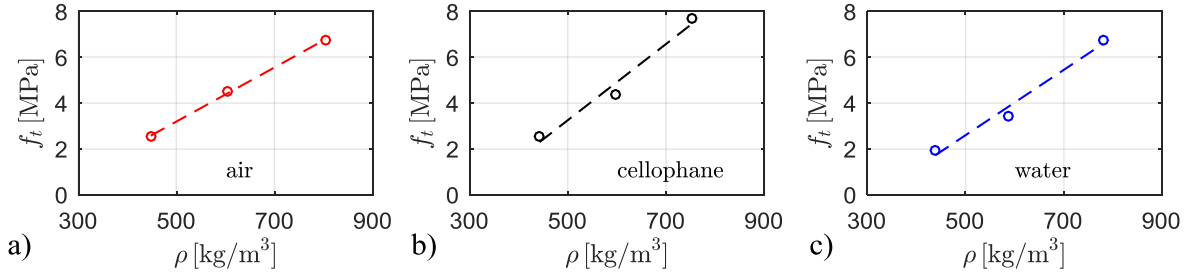

Fig. 18. Experimental indirect tensile strength for foamed concrete beams with glass-fiber grids combined with short polymer fibers (2% in volume) and different curing conditions: a) air; b) cellophane; c) water.

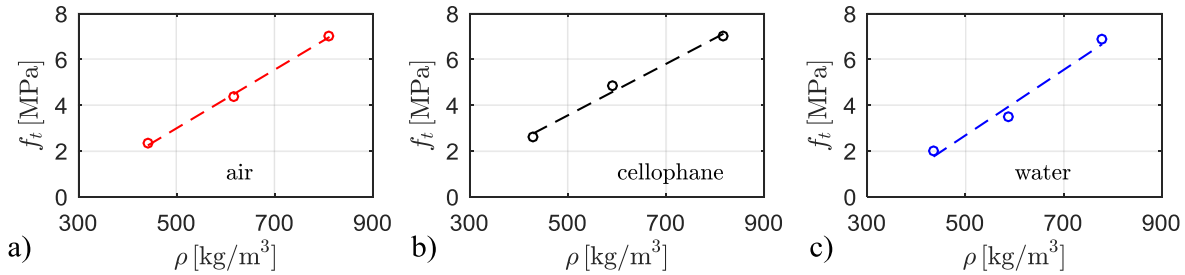

Fig. 19. Experimental indirect tensile strength for foamed concrete beams with glass-fiber grids combined with short polymer fibers (5% in volume) and different curing conditions: a) air; b) cellophane; c) water.

Table 8
Experimental indirect tensile strength and compressive strength for specimens with glass-fiber grids combined with short polymer fibers (5% in volume).

curing conditions	series no.	dry density γ_{dry} [kg/m^3]	rupture tensile strength f_t [MPa]	compressive strength R_c [MPa]
air	#1GF5	441	2.32	n.a.†
	#2GF5	617	4.34	n.a.†
	#3GF5	811	7.05	11.02
cellophane	#4GF5	429	2.62	n.a.†
	#5GF5	591	4.82	5.38
	#6GF5	817	7.02	12.83
water	#7GF5	435	2.01	n.a.†
	#8GF5	587	3.46	n.a.†
	#9GF5	778	6.86	9.01

† Not available result due to the collapse mode in three-point-bending test that has affected also both the halves of the corresponding beams to be used for the compression test.

equal to around 175%. It is not easy to compare the obtained results with other research studies from the relevant literature. In fact, to the authors' best knowledge, only one work dealt with the use of bi-directional reinforcement grids (of basalt fiber grid and carbon fiber grid, thus of different nature with respect to the adopted glass fibers of the present study) to enhance the flexural capacity of foamed concrete slabs [27]. The significant increase of flexural capacity induced by the bi-directional reinforcement grid is confirmed by the mentioned study [27]. These authors reported values of the flexural strength of three-point-bending tests of around 2 MPa for a density nearly equal to 800 kg/m^3 [27]. This value is lower than the result obtained in the present experimental campaign for a comparable dry density of 800 kg/m^3, which is around 5 MPa. This is justifiable in view of the different mechanical characteristics of the foamed concrete material used, as the compressive strength reported in [27] was lower than 2 MPa, whereas our results indicate nearly 12 MPa, cf. specimen #3U in Table 5.

The further addition of the short polymer fibers leads to a modest improvement as compared to the previous reinforcement arrangement, except for the higher dry densities. In the latter density configurations, the lower porosity of the specimens (corresponding to a higher solid phase within the specimen) enhances the strength contribution offered by the fibers as they interact more effectively with the surrounding concrete matrix. This is clearly seen for all the curing conditions. On the contrary, for lower densities (e.g. 400–600 kg/m^3) the further increase of the tensile strength due to the addition of fibers is rather negligible. In earlier experimental studies, the effect of different contents of fibers (ranging from 0.2% to 1.5%) on the flexural capacity of foamed concrete was investigated [19–21]. In particular, in [37] the use of poly vinyl alcohol (PVA) fibers in 1% volume content led to flexural strength gain of around 160%, passing from 0.74 MPa to 1.92 MPa for a density of around 850 kg/m^3. In the present study, the use of polymer fibers in 2% volume content combined with bi-directional glass fiber reinforced grid led to a 215% flexural strength gain, passing from 2.15 MPa to 6.75 MPa in air curing conditions for a target dry density of 800 kg/m^3. These comparisons highlights two important aspects: 1) the extrudable foamed concrete material used in this experimental campaign presents better strength characteristics in comparison with other literature studies; 2) the major contribution to the increase of the flexural capacity seems to be offered by the bi-directional glass fiber grids rather than by the short fibers. Considering the applications envisaged for this material in non-structural components and partition walls of buildings that may require strength values not very high but, at least, higher than 1.5 MPa

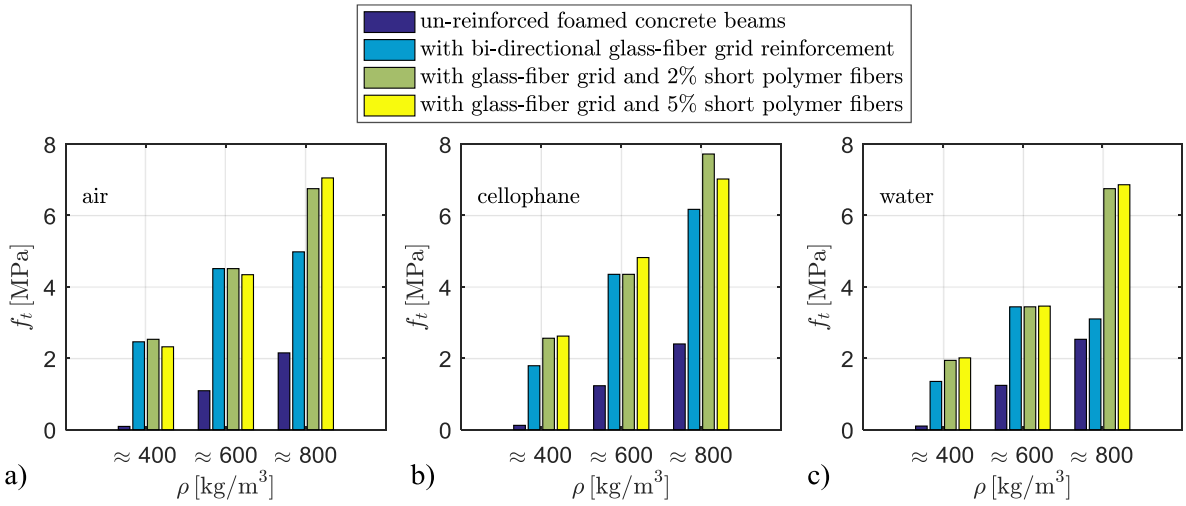

Fig. 20. Comparative histograms of indirect tensile strength values for different reinforcement strategies of the foamed concrete beams, for different target dry densities and curing conditions in: a) air; b) cellophane; c) water.

Fig. 21. Photographs at failure of foamed concrete beams cured in cellophane: a) close-up detail at the mid-span beam soffit; b) interaction between short polymer fibers and glass-fiber bi-directional grid reinforcement; c) detail of the rupture zone with concrete detachment.

for compression strength and 0.2 MPa for flexural strength, the following conclusions can be drawn. For unreinforced foamed concrete, densities equal to or higher than 500 kg/m^3 are necessary to meet the above minimum requirements; instead, for foamed concrete reinforced with bi-directional grids, also lower densities (400 kg/m^3) can be employed for this kind of applications.

Some photographs taken at failure of the beams are illustrated in Fig. 21, which highlights the combined effect of the short polymer fibers in conjunction with glass-fiber bi-directional grid reinforcement. It is noted that the collapse mechanisms of these reinforced beams resemble the ones shown before in Fig. 13, with the concrete cover separating from the remaining portion of the beam due to the attainment of the bond strength at the interface. For the specimens shown in Fig. 21 the bi-directional grid does not exhibit a premature rupture since the illustrated beams were cured in cellophane. On the contrary, for beams cured in water the same phenomena noted in Fig. 14 were observed. However, even for these beams at higher dry densities (800 kg/m^3) the indirect tensile strength value is considerably higher than the ones discussed in Section 4 with only grid reinforcement without short fibers. This suggests that the above-mentioned interaction effects between the two levels of reinforcement effectively took place to enhance the ultimate flexural capacity of the beams when the foamed concrete is endowed with good inherent strength features typical of higher dry densities.

7. Concluding remarks

In this work, an experimental campaign comprising almost 40 small-scale foamed concrete beams has been conducted to investigate the possibility of increasing the flexural capacity with different reinforcement arrangements. The flexural capacity has been investigated under different curing conditions of the specimens, and for different dry densities mostly focused in the low-to-medium range. First, a set of unreinforced specimens were prepared for reference purposes. Then, some additional specimens were prepared and reinforced with three alternative strategies to improve the flexural capacity, namely: 1) glass-fiber bi-directional grids placed in the tensile zone of the beams; 2) combined glass-fiber grids with short polymer fibers, the latter being embedded within the cementitious paste at a volume content of 2%; 3) the same reinforcement arrangement as in 2) but with a higher volume content of polymer fibers, namely equal to 5%.

The main results of this experimental investigation are summarized as follows:

- the presence of the glass-fiber bi-directional grid improved the flexural capacity of the foamed concrete beams for all the analyzed configurations (densities and curing conditions);
- the increase of flexural capacity is enormous for the specimens with very low dry densities (400 kg/m^3), reaching an average value of more than 1780% as compared to the un-reinforced beams: this suggests that the proposed reinforcement strategy is an effective method for obtaining an offset between ultra-lightweight properties (due to the low density) and acceptable strength characteristics that cannot be achieved at such low densities; without such reinforcement the tensile strength values are really low for these ultra-lightweight elements;
- the increase of flexural capacity is significant also for low-medium dry densities of 600 kg/m^3 and 800 kg/m^3 analyzed in this study, although not as dramatic as in the lowest dry densities of 400 kg/m^3. For this higher density range the increase is dependent upon the curing conditions: in air of 223%, in cellophane 205%, in water 99%, on average;
- the lower strength increase observed in water was due to the degradation of the mechanical characteristics of the grid induced by the water curing conditions;
- the collapse mechanism of the foamed concrete beams is also affected by the curing conditions: in water, a premature rupture of the grid at the mid-span soffit of the beam at ultimate conditions was observed, while the other beams exhibited typical bond failure with detachment of concrete substrate from reinforcement;
- the further addition of short polymer fibers led to a modest increase of the flexural capacity both at the 2% and 5% volume content for almost all the tested specimens except for higher dry densities (800 kg/m^3) – this fact is consistent with a more effective interaction of the short fibers with a denser cementitious matrix;
- following the previous bullet point, it has been observed that while the introduction of a 2% fiber content does increase the flexural capacity (in comparison with the grid reinforcement only) at higher densities, a further increase to 5% does not produce considerable improvements. Based on these outcomes and considering the optimal offset between costs and performance, it is recommended to limit the fiber content in foamed concrete elements to within 2% in volume if the same characteristics of the specimens as in this experimental campaign are adopted.

The present investigation is just a preliminary experimental study limited to small-scale specimens, but is part of a wider research program including large-scale walling systems. Through the proposed reinforcement strategies higher strength values may be obtained with relatively low densities, the latter assuring a lower self-weight of the structure as a whole, a good thermal insulating performance due to the internal void presence in the microstructure, and impermeability features. Furthermore, the extrusion process of this new material might speed up the construction processes of structural and non-structural elements in the framework of 3D printing applications and, thus, lower the implied costs.

The applicability of this new material in the construction industry requires a more comprehensive study of all the engineering properties, not just limited to the mechanical characteristics, but also including fresh-state properties, physical (especially with regard to drying shrinkage that may be a major issue for practical applications), microstructural and durability features, which are not included in this

paper but are object of ongoing experimental investigations. Further study will focus on the extension of the investigation to higher dry densities so as to confirm the concluding remarks outlined above, and the analysis of other fiber contents and reinforcement configurations, for instance, the presence of short polymer fibers only without bi-directional reinforcement mesh.

Acknowledgements

The authors wish to thank the company Colacem S.p.A. for supplying the cement Portland CEM I 52,5 R necessary for this experimental work.

Data availability statement

The data that support the findings of this study are available from the corresponding author, DDD, upon reasonable request.

References

[1] Ramamurthy K, Nambiar EK, Ranjani GIS. A classification of studies on properties of foam concrete. Cem Concr Compos 2009;31(6):388–96.
[2] Faleschini F, Fernández-Ruíz MA, Zanini MA, Brunelli K, Pellegrino C, Hernández-Montes E. High performance concrete with electric arc furnace slag as aggregate: mechanical and durability properties. Constr Build Mater 2015;101:113–21.
[3] De Domenico D, Faleschini F, Pellegrino C, Ricciardi G. Structural behavior of RC beams containing EAF slag as recycled aggregate: numerical versus experimental results. Constr Build Mater 2018;171:321–37.
[4] Jones MR, McCarthy A, Dhir RK. Recycled and secondary aggregate in foamed concrete. Banbury, Oxon OX16 0AH: WRAP Research report, the waste and resources action programme; 2005.
[5] Yang KH, Lee KH, Song JK, Gong MH. Properties and sustainability of alkali-activated slag foamed concrete. J Cleaner Prod 2014;68:226–33.
[6] Wei S, Yiqiang C, Yunsheng Z, Jones MR. Characterization and simulation of microstructure and thermal properties of foamed concrete. Constr Build Mater 2013;47:1278–91.
[7] Valore RC. Cellular concrete part 2 physical properties. ACI J 1954;50:817–36.
[8] Tada S. Material design of aerated concrete-an optimum performance design. Mater Constr 1986;19:21–6.
[9] Nambiar EKK, Ramamurthy K. Fresh state characteristics of foam concrete. ASCE Mater Civ Eng 2008;20:111–7.
[10] Falliano D, De Domenico D, Ricciardi G, Gugliandolo E. Experimental investigation on the compressive strength of foamed concrete: effect of curing conditions, cement type, foaming agent and dry density. Constr Build Mater 2018;165:735–49.
[11] Decký M, Drusa M, Zgútová K, Blaško M, Hájek M, Scherfel W. Foam concrete as new material in road constructions. Procedia Eng 2016;161:428–33.
[12] Kadela M, Kozłowski M. Foamed concrete layer as sub-structure of industrial concrete floor. Procedia Eng 2016;161:468–76.
[13] Othuman Mydin MA, Wang YC. Structural performance of lightweight steel-foamed concrete–steel composite walling system under compression. Thin-Walled Struct 2011;49(1):66–76.
[14] Jones MR, Ozlutas K, Zheng L. Stability and instability of foamed concrete. Mag Concr Res 2016;68(11):542–9.
[15] Jones MR, Ozlutas K, Zheng L. High-volume, ultra-low-density fly ash foamed concrete. Mag Concr Res 2017;69(22):1146–56.
[16] Tam CT, Lim TY, Sri Ravindrarajah R, Lee SL. Relationship between strength and volumetric composition of moist-cured cellular concrete. Mag Concr Res 1987;39(138):12–8.
[17] Long WW, Wang JS. Study on Compressive Strength and Moisture Content of Different Grades Density of Foam Concrete. In: International Conference on Material Science and Application (ICMSA 2015). DOI: 10.2991/icmsa-15.2015.32.
[18] Thakrele MH. Experimental study on foam concrete. Int J Civ Struct Environ Infrastruct Eng Res Dev 2014;4(1):145–58.
[19] Bing C, Zhen W, Ning L. Experimental research on properties of high-strength foamed concrete. J Mater Civ Eng 2011;24(1):113–8.
[20] Kayali O, Haque MN, Zhu B. Some characteristics of high strength fiber reinforced lightweight aggregate concrete. Cem Concr Compos 2003;25(2):207–13.
[21] Sun HY, Gong AM, Peng YL, Wang X. The study of foamed concrete with polypropylene fiber and high volume fly ash. Applied Mechanics and Materials, vol. 90. Trans Tech Publications; 2011. p. 1039–43.
[22] Awang H, Ahmad MH. Durability properties of foamed concrete with fiber inclusion. World Acad Sci Eng Technol Int J Civ Environ Struct Constr Arch Eng 2014;8(3):273–6.
[23] Mahzabin MS, Hock LJ, Hossain MS, Kang LS. The influence of addition of treated kenaf fibre in the production and properties of fibre reinforced foamed composite. Constr Build Mater 2018;178:518–28.
[24] Lee JH. Influence of concrete strength combined with fiber content in the residual flexural strengths of fiber reinforced concrete. Compos Struct 2017;168:216–25.
[25] Niaki MH, Fereidoon A, Ahangari MG. Experimental study on the mechanical and thermal properties of basalt fiber and nanoclay reinforced polymer concrete. Compos Struct 2018;191:231–8.
[26] Chen J, Chouw N. Flexural behaviour of flax FRP double tube confined coconut fibre reinforced concrete beams with interlocking interface. Compos Struct 2018;192:217–24.
[27] Hulimka J, Krzywoń R, Jędrzejewska A. Laboratory tests of foam concrete slabs reinforced with composite grid. Procedia Eng 2017;193:337–44.
[28] Rum RHM, Jaini ZM, Ghaffar NA, Rahman NA. A preliminary experimental study on vibration responses of foamed concrete composite slabs. IOP Conf Ser: Mater Sci Eng 2017;271(1):012102.
[29] De Sutter S, Verbruggen S, Tysmans T, Aggelis DG. Fracture monitoring of lightweight composite-concrete beams. Compos Struct 2017;167:11–9.
[30] Portal NW, Flansbjer M, Zandi K, Wlasak L, Malaga K. Bending behaviour of novel Textile Reinforced Concrete-foamed concrete (TRC-FC) sandwich elements. Compos Struct 2017;177:104–18.
[31] Panesar DK. Cellular concrete properties and the effect of synthetic and protein foaming agents. Constr Build Mater 2013;44:575–84.
[32] Falliano D, De Domenico D, Ricciardi G, Gugliandolo E. Mechanical characterization of extrudable foamed concrete: an experimental study. World Acad Sci Eng Technol Int J Civ Environ Eng 2018;12(3):228–32.
[33] Falliano D, Gugliandolo E, De Domenico D, Ricciardi G. Experimental investigation on the mechanical strength and thermal conductivity of extrudable foamed concrete and preliminary views on its potential application in 3D printed multilayer insulating panels. First RILEM International Conference on Concrete and Digital Fabrication – Digital Concrete 2018. Cham: Springer; 2019. p. 277–86. DOI: 10.1007/978-3-319-99519-9_26.
[34] Jones MR, McCarthy A. Preliminary views on the potential of foamed concrete as a structural material. Mag Concr Res 2005;57(1):21–31.
[35] Xu Z, Chen Z, Yang S. Effect of a new type of high-strength lightweight foamed concrete on seismic performance of cold-formed steel shear walls. Constr Build Mater 2018;181:287–300.
[36] Cebeci ÖZ. Pore structure of air-entrained hardened cement paste. Cem Concr Res 1981;11(2):257–65.
[37] Meyer D, Van Mier JGM. Influence of different PVA fibres on the crack behaviour of foamed cement paste. Proceedings of sixth international conference on 'fracture mechanics of concrete structures'. London: Taylor & Francis Group/Balkema; 2007. p. 1359–65.